Studying The Effect of The Manufacturing Process of Heusler Compounds Co_2MnZ (Z=Ga, Ge, Si) on its Crystal Order and Magnetic Properties

Hamayoon, Rahmani*; Mohammad Jawad Hamta, Ibrahim Tawana, Hussain Aziz
Department of Physics, Faculty of Natural Science, Bamyan University, Afghanistan
*Corresponding Author: *hamayoonrahmani1990@gmail.com*

Received: 13 September 2022; **Accepted**: 17 October 2022; **Published**: 12 November 2022
DOI: http://dx.doi.org/10.29303/jpft.v8i2.4048

Abstract - *The effect of different manufacturing processes, such as arc melting, mechanical alloying, and baking, on the crystalline and magnetic behavior of Co_2MnSi, Co_2MnGa, and Co_2MnGe compounds was investigated. Samples of Co_2MnSi, Co_2MnGe, and Co_2MnGa compounds were produced using the arc melting method and the effect of mechanical alloying and annealing processes on the manufactured products was investigated. The results showed that the use of different processes during manufacturing leads to different crystalline and magnetic behaviors of the sample. One of these cases is the correlation of the crystal order with the lattice parameter size in the produced samples and its effect on reducing the saturation magnetization compared to Slater and Pauling's prediction. Also, the change of order induced by the mechanical alloying process in the production of Co_2MnSi composition has led to a drop of about 14% in saturation magnetization. The coercivity in the sample produced by arc melting and mechanical alloying in Co_2MnGe composition is lower than the expected value, which was attributed to the low magnetic anisotropy of the sample due to the small size of the crystals in this sample, which is compensated in the cooking process. For example, performing the grinding process before baking leads to a change in the crystal order and, consequently, to a decrease in the saturation magnetization of the sample. The final baking increases the size of the crystals and reduces the strain. The sample obtained from grinding after arc melting had more coercivity than the other two samples due to having smaller crystals.*

Keywords: *Heusler; Crystal Order; Magnetic Properties; Mechanical Alloying; Arc Melting.*

INTRODUCTION

Heusler compounds are a group of magnetic materials that have attracted a lot of attention due to their diverse properties such as magneto-optic properties(Gani et al., 2021), magnetic memory(Graf et al., 2011), magnetothermal behavior(Webster et Ziebeck, s. d.), thermoelectricity(Yin et al., 2015), etc. Also, large spin polarization, high Curie temperature, ability to grow easily in the form of a thin film, and special half-metal properties in cobalt-based Heusler alloys have recently attracted the attention of many researchers(Miura et al., 2004).

The magnetic moment of Cobalt-based Heusler compounds is in good agreement with the Slater-Pauling relationship, and in the meantime, the saturation magnetization is predicted to be 5 $\mu_B/_{F.u.}$ for the Heusler compounds Co_2MnSi and Co_2MnGe, which have 29 valence electrons per formula unit(Graf et al., 2011). Among known Heusler compounds, the Co_2MnSi compound has the highest Curie temperature (Campbell, 1976). Also, due to the energy gap of about 0.4 eV in a spin direction, it plays an important role in spintronic applications(Knowlton et Clifford, 1912).

Obtaining high spin polarization in Heusler Co_2MnGe ferromagnetic alloy requires a high degree of crystal order $L2_1$. For this composition, a high Curie temperature of

905K has been reported. This compound is one of the intermetallic compounds that maintain the $L2_1$ order up to the melting temperature(Collins et al., 2015). Co_2MnGa is one of the Heusler compounds of cobalt base, which has 28 valence electrons. Slater and Paulinck's model gives the value of saturation magnetization for this combination of 4 μ_B/F.u. Recently, Co_2MnGa alloy has attracted special attention as its usefulness as a spin-injection layer in spintronic devices operating at room temperature (RT) has been demonstrated(Holmes et Pepper, 2002).

R. J. Kim et al. found a well-ordered crystalline state, a disordered state, and a crystalline state with an intermediate order and exhibited the influence of structural order on the physical properties of Co2MnGa films(Kim et al., 2006).

In the meantime, the research conducted on similar compounds shows that the production method of affecting the microstructure and the possibility of changing the anisotropy caused by the crystalline behavior of the material can significantly change the magnetic quantities which in the case of these compounds. So far, less attention has been paid to this issue (Nazari et al., s. d.). Therefore, in this research, the effects of the production method on the microstructural characteristics and consequently the magnetic quantities of this compound are considered.

RESEARCH METHODS

Materials and method of testing Co_2MnSi, Co_2MnGe, and Co_2MnGa compounds

Samples of Co_2MnSi, Co_2MnGe, and Co_2MnGa compounds were produced using the arc melting method and the effect of mechanical alloying and annealing processes on the manufactured products was investigated. For this purpose, at first, prototypes were produced during the arc melting process in the argon atmosphere by passing current (125A). In the next step, a series of these samples were mechanically alloyed under an argon atmosphere for 15 hours, which was named S_{am}. Next, a part of these samples was annealed for 48 hours at 800 °C in a vacuum environment and was named S_{ama}. Other samples produced by arc melting without mechanical alloying were baked for 48 hours at 800 °C and named S_{aa}.

The crystal structure of the samples was investigated by X-ray diffraction (XRD) using a Philips PW1730 device with a copper lamp with a wavelength of 0.154 nm. Williamson-Hall relation was used to calculate the grain size and network strain. XRD data were analyzed using Full Prof software based on the Rietveld method. Scanning Electron Microscope (SEM) model 30 Philips, XL was used to check the microstructure of the produced samples. Also, a Lakeshore Model Vibrating Sample Magnetometer (VSM) was used to check the magnetic properties of the samples produced at ambient temperature.

RESULTS AND DISCUSSION

The results of the X-ray diffraction analysis of the samples produced with the simulated beam using the Rietveld method are shown in Figure 1. As can be seen, the peaks in all five samples correspond to the structural peaks of the cubic crystal with the space group Fm-3m, which is characteristic of Heusler compounds. In these figures, the red curve corresponds to the experimental data of the XRD spectrum. The black curve shows the calculated spectrum adapted by Rietveld software, the blue graph shows the difference between the two experimental and calculated spectra, and the green lines show the position of the Bragg peaks. The presence of high-

intensity peaks in S_{ama} and S_{aa} samples of Co_2MnSi composition indicates the crystallization of the material.

In the case of the S_{am} sample, only a few broad peaks can be seen in this composition. Except for the peak located at 44 degrees, the height of the other peaks is of the order of the background fluctuations of the spectrum, and this indicates weak crystallinity and the presence of relatively high residual stresses from the mechanical alloying stage in this sample. The weak crystallinity of this sample can lead to weak atomic magnetic order. The difference in the width of the XRD peaks is attributed to the size of the crystals and the internal strain of the network. The change of these two quantities affects the movement mechanism of the domain wall in the magnetization and demagnetization processes.

The effects of long-range crystal order in S_{aa} and S_{ama} samples of Co_2MnSi composition have appeared in the form of superlattice peaks. The Sam sample of Co_2MnGe composition with the S_{am} sample of Co_2MnGa composition seems completely different in terms of the intensity of the width and the number of peaks as well as the background fluctuations. In the S_{am} sample of Co_2MnGe composition, the peaks appeared with relatively greater intensity and less width, which can be related to the larger crystal size in the S_{am} sample of Co_2MnGe composition. Still, the S_{am} sample of Co_2MnGa composition has more noise than other samples, which shows the weak crystallinity of this sample.

All S_{am} samples of these compounds have been produced in a similar way but with different characteristics. In particular, unconventional growth is observed for the Co_2MnGe composition compared to the other two compositions. The comparison of the crystal order of the compounds is done by examining the peaks of the superlattice at the angles of and, based on this, it is not possible to comment on the state of the crystal order of the three S_{am} samples because it is difficult to separate these peaks from the fluctuations of the background. Another way to check the crystal order is to study the difference in the relative height of the peaks, which can be due to the difference in the arrangement of cations in the cubic structure. From this point of view, no specific difference can be distinguished between the three samples of S_{am}.

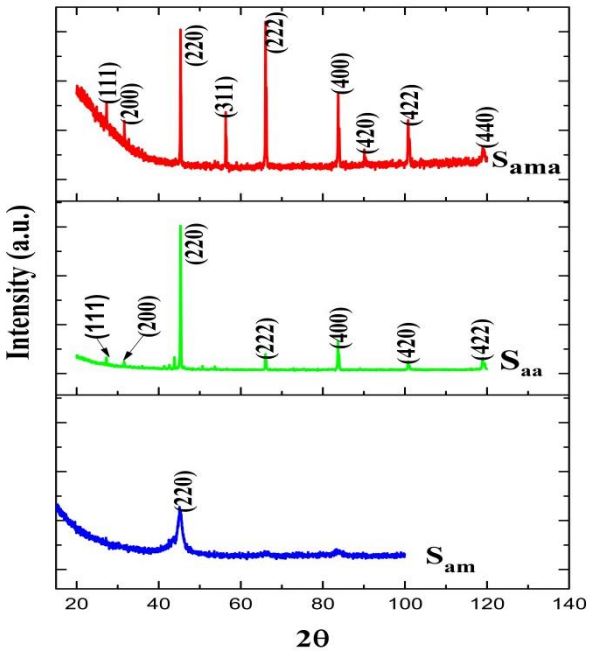

Figure 1. XRD patterns of the produced samples.

The parameters of the crystal lattice of the samples obtained by the Rietveld simulation are presented in Table 1. The largest lattice parameter in the Co_2MnSi composition is related to the S_{am} milled sample with a value of 5.68 Å. The lattice parameter has decreased to 5.65 Å during the baking process and this quantity is equal to 5.66 Å in the S_{aa} sample.

Lattice parameters (5.67 Å) have been reported in the articles for a volumetric sample of Co_2MnSi, with a cubic L21 structure

(Gubin et al., 2005). Also, Galenkis and his colleagues have calculated the network parameter as 5.65Å (Şaşıoğlu et al., 2005). The importance of this quantity is that for a specific crystal order, the length of bonds between atoms is directly related to the lattice parameter. On the other hand, the exchange constant in the exchange interaction between atoms can change by changing the distance. According to the model of Slater-Pauling, 3D elements have antiferromagnetic interaction at small distances. As the distance increases, this interaction weakens and turns into ferromagnetic interaction. As the distance increases, the strength of the interaction increases up to a certain distance and then decreases (Varaee et al., 2021).

The lattice parameter (5.97 Å) of the S_{am} sample composed of Co_2MnGa is larger than the lattice parameter (5.76 Å) of the S_{am} sample composed of Co_2MnGe, which can be due to the larger atomic radius of Ga compared to Ge. The atomic radius values of Ga and Ge in picometers are 136 and 125, respectively. The largest lattice parameter calculated in these compounds is related to the S_{am} sample of the Co_2MnGa compound with a value of 5.97 Å, which decreased to 5.75 Å during the baking process. The reduction of lattice parameters during the baking process is similar to the behavior seen in Co_2MnSi samples.

Here too, this change may be attributed to the change in the crystal order of the sample. The lattice parameter of the other two samples in these compounds is slightly smaller than this value. Using the generalized gradient approximation (GGA), Magan et al obtained a lattice parameter of 5.74 Å for the Co_2MnGe compound (Ido, 1986). Using the LDA+U approximation, Kandpal et al obtained the lattice parameter for the 5.76ÅCo_2MnGa compound (Kandpal et al., 2007).

The average size of the crystals and the lattice strain are calculated from the Williamson-Hall relationship relation 1 and presented in table (1).

$$B\cos\Theta=K\lambda/D+2\varepsilon\sin\Theta \quad (1)$$

Where D is the average size of the crystals, B is the half-width of the peak, Θ is the Bragg angle of the peak, ε is the strain, K is constant, and λ is the wavelength of the X-ray.

Based on the core and shell model, the size of the crystals can affect the saturation magnetization of the samples. In addition, the change in the size of the crystals affects the coercivity of the sample (Mahaux et al., 1985). Generally, the coercivity increases with the decrease in the size of the crystals; this increase continues until reaching the superparamagnetic range, and then the coercivity decreases due to the single domain of the crystal grains (Phong et al., 2022). On the other hand, network strain can also affect coercivity. The occurrence of strain is effective in the mechanism of producing reverse magnetic domain walls and also in the movement of domain walls. Usually, increasing the strain increases the coercivity (Caizer, 2016).

The largest crystal size calculated in the composition of Co_2MnSi corresponds to the S_{aa} sample with a value of 61 nm, which indicates the growth of the crystals due to the re-baking process in this sample after the arc melting stage. In fact, due to the exposure of this sample to high temperatures, a suitable substrate has been provided for their growth and their size has increased. Also, the crystal lattice strain in the S_{am} milled sample is larger

than that in other samples, which seems reasonable considering the impact of the bullet during the milling process. S_{aa} and S_{ama} samples of the Co_2MnSi composition have the s_{ame} strain equal to 0.05% and, due to the different atomic radii of the constituent elements of the composition, the atomic disorder can also affect the crystal lattice strain (Fariba et al., 2015).

Table 1. Structural parameters of the samples

Compounds	Sample	Crystal structure	lattice parameter(Å)	space group	Crystal size(nm)	Strain (%)
Co_2MnSi	S_{am}	cubic	5.68	Fm-3m	10	0.07
	S_{ama}	cubic	5.65	Fm-3m	58	0.05
	S_{aa}	cubic	5.66	Fm-3m	61	0.05
Co_2MnGa	S_{am}	cubic	5.76	Fm-3m	30	0.09
Co_2MnG	S_{am}	cubic	5.97	Fm-3m	8	0.05
	S_{ama}	cubic	5.75	Fm-3m	60	0.02

The point is that the size of the crystal is larger in the S_{am} sample of Co_2MnGe composition compared to Co_2MnGa. SEM images of S_{am} and S_{ama} samples of these compounds are shown in Figure (2). The distribution of particle size in the S_{am} sample of these compounds is relatively uniform and the shape of the particles is observed symmetrically.

In some areas of the image, traces of the agglomeration of particles can be seen. This behavior can be caused by the cold boiling of the produced particles due to the impact of the balls during milling. The SEM image of S_{ama} sample of Co_2MnSi composition also indicates a powder structure with particles with symmetrical shapes. The size of the particles in this sample is similar to sample S_{am} and is in the order of microns and above microns.

Here too, the particles have accumulated in some areas, and the agglomeration behavior is much more observed in them compared to the sample S_{am}. Agglomeration can be strengthened by strengthening the bonding of grains in the cooking process. The SEM image of the surface of the particles on a finer scale shows the same behavior as the S_{am} sample, with the difference that the average dimensions of the grains have grown in this sample. Also, the connection of grains is strengthened in this sample. Meanwhile, in the S_{ama} sample of the Co_2MnGa composition, the entanglement of particles has increased greatly. The symmetry of the particles that were seen in the previous three samples is not observed here. This behavior can induce a kind of magnetic anisotropy due to the shape of the particles.

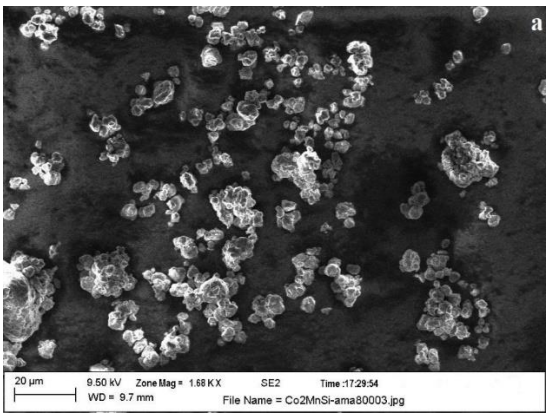

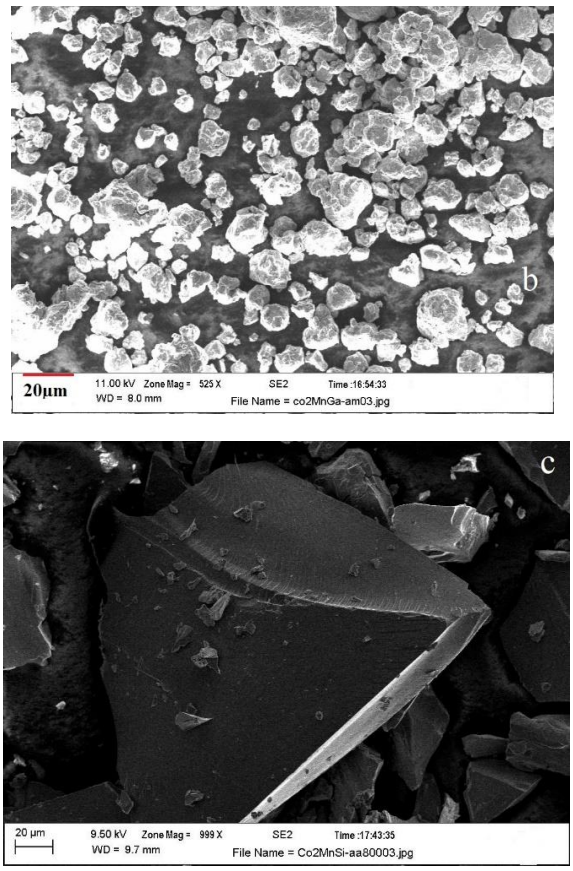

Figure 2. SEM images of samples: a) S_{ama}, b) S_{am} and c) S_{aa}.

The magnetic hysteresis loop of samples of Co_2MnSi, Co_2MnGe, and Co_2MnGa compounds at ambient temperature is shown in Figure 3. To see the details of the central part of the hysteresis loop, it is drawn on a larger scale in the inset of this figure. Also, the values of saturation magnetization in terms of magneton-Bohr per chemical formula unit are calculated with the purpose of comparison with the Slater-Pauling model and, together with other quantities obtained from the residual loop of the samples, are shown in Table 2.

The magnetization of all the samples is greatly increased by applying a small field and reaching the saturation limit, and this property is related to soft magnetic materials. Also, the obliqueness of the residual loops indicates a strong drop in magnetization with the removal of the magnetic field (Wang, 2010). The saturation magnetization of S_{aa} sample of Co_2MnSi composition is greater than that of the other two samples and is equal to 5.13 μ_B/F.u. which is from the expected value of 5μ_B/F.u. The Slater-Pauling model is slightly larger for this combination. This quantity in the experimental works of others between $4.9\frac{\mu_B}{F.u.}$ (Kämmerer et al., 2004) and $5.3\frac{\mu_B}{F.u.}$ (Raphael et al., 2002) is variable. As seen in the XRD patterns, there was a relative difference in the height of the peaks of the two samples, S_{ama} and S_{aa} of Co_2MnSi composition, which is due to the difference in their crystal orders.

The difference in the saturation magnetization values of these two samples can also be explained based on the same difference in crystal order. But in the S_{am} sample, which has the same crystal order as S_{aa}, a saturation magnetization drop has also been observed, and the origin of this difference can be found in the difference in the size of the crystals of these two samples according to the core and shell model.

Table 2. Magnetic parameters of the samples.

Compounds	Sample	$M_s(\mu_B/F.u.)$	$M_s(Am^2/kg)$	$H_c(Oe)$	$M_r(Am^2/kg)$
Co_2MnSi	S_{am}	4.41	116	7.32	5.22
	S_{ama}	4.16	113	1.64	1.00
	S_{aa}	5.13	142	1.38	1.06
Co_2MnGa	S_{am}	3.48	81	2.72	1.33
	S_{ama}	4.28	99	2.66	1.57
	S_{aa}	3.17	86	2.69	1.50
Co_2MnGe	S_{am}	2.99	69	7.37	3.42
	S_{ama}	3.62	83	1.40	0.46
	S_{aa}	4.90	112	1.76	0.86

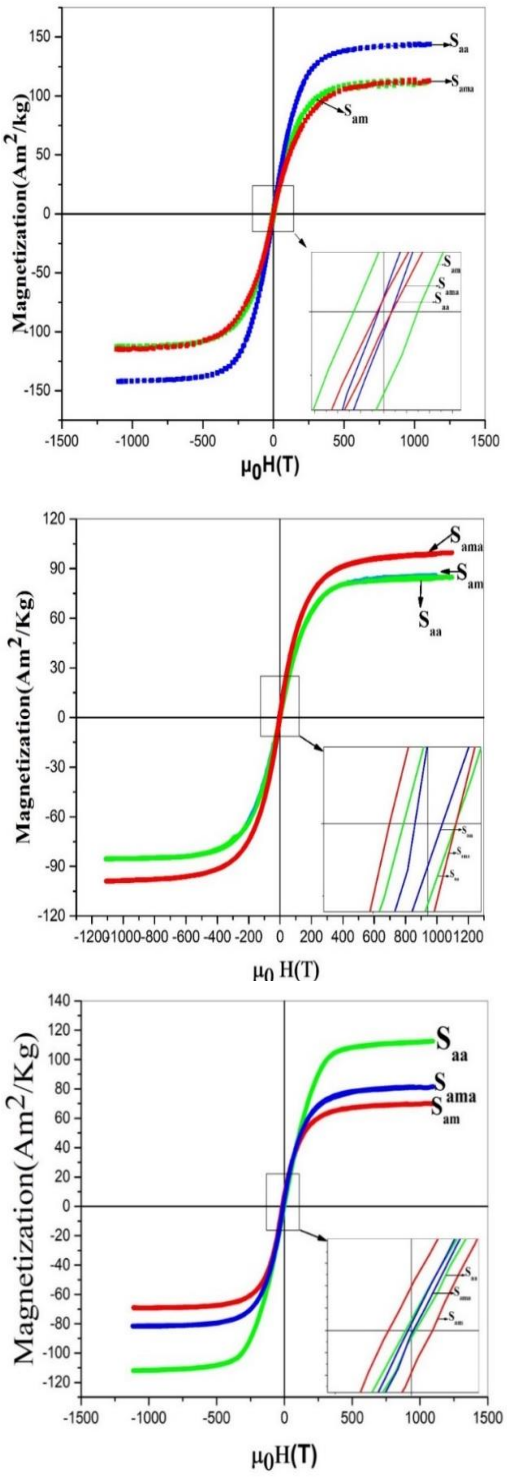

Figure 3. Magnetic hysteresis curves of Co2MnSi, Co2MnGa, and Co2MnGe composition samples.

The largest value of coercivity in the composition of Co_2MnSi for the S_{am} sample is 7.32Oe. Meanwhile, the amount of this quantity in the cooked sample is greatly reduced. As determined from the XRD results, the growth of the grain size and, consequently, the weakening of the grain boundary effect as well as the reduction of the lattice strain can be mentioned as the main reasons for the reduction of the coercive field by affecting the mechanism of creating the wall of the magnetic domains and their mobility.

The reduction of coercivity with increasing grain size is known to be due to the reduction of surface irregularities. The amount of M_r in the S_{am} sample of this composition equals 5.22 Am^2/kg, which is the highest value, which can be related to the high coercivity of this sample. In the S_{aa} sample of Co_2MnGa composition, the saturation magnetization of 86 Am^2/Kg was obtained, which is equivalent to $3.71 {}^{\mu_B}/_{F.u.}$. This value is slightly less than Slater and Pauling's prediction. This decrease in magnetization is caused by factors such as the samples not being single crystal, structural twist, and crystal disorder in the manufactured samples(Kobayashi et al., 2004).

The presence of impurities and possible stoichiometric changes due to partial evaporation of the samples can be considered as a double reason for the decrease in saturation magnetization, although the change in the crystal order and the size of the lattice parameter may also be effective in the smallness of this quantity. The remarkable thing is that a significant increase in the saturation magnetization of the S_{ama} sample is observed from this composition so that the value of this quantity has reached from $3.48 {}^{\mu_B}/_{F.u.}$. For the S_{am} sample to $4.28 {}^{\mu_B}/_{F.u.}$. Another point that can be seen in these data is the closeness of coercivity of S_{am} and S_{ama} samples in this composition, which is

due to the growth of grain size and reduction of strain during baking, the root of this behavior can be found in the change of anisotropy of the two samples.

As seen in the SEM images, the occurrence of some form of anisotropy in the particles of this sample is not far from expected. In addition, due to the unconventional increase of the saturation magnetization in this sample, the anisotropy of the Nir crystal magneto may have been enhanced.

The saturation magnetization of an S_{aa} sample of Co_2MnGe composition is greater than that of the other two samples and is equal to 112 Am^2/kg. This value is equivalent to $4.90 {}^{\mu_B}/_{F.u.}$, which is slightly smaller than the expected value of $5.5 {}^{\mu_B}/_{F.u.}$ of the Slater-Pauling model for this composition. It seems that reasons such as thermal fluctuations of torques and non-stoichiometric effects can be mentioned for the low measured saturation magnetization (Margulies et al., 1996). In addition, there are reports of the existence of a phase separation phenomenon in cobalt-based Heusler compounds (Felser et Seshadri, 2000). According to these reports, the co-existence of phases with different crystal irregularities in some Heusler compounds is inevitable and can be the main reason for this difference. In addition, the fact that the sample is not a single crystal can also be mentioned as a reason for the low saturation magnetization compared to the predictions of Slater and Pauling.

CONCLUSION

The results of this research confirmed the formation of a cubic crystal structure for all the produced samples. The milled sample without baking had the lowest crystallinity. Also, due to the difference in the arrangement of atoms in different samples, the relative heights of the peaks were very different.

According to the SEM images, two samples made by the grinding method showed particles with different appearances and smaller particle sizes compared to the unground sample.

According to the magnetic remanence loop, the saturation magnetization in the sample obtained from arc melting product firing was greater than the value predicted by the Slater-Paulinck model. Due to the presence of smaller crystal grains in the sample made by the arc melting method, the coercivity quantity has the highest value.

REFERENCES

Caizer, C. (2016). Nanoparticle size effect on some magnetic properties. *Handbook of Nanoparticles*, 475.

Campbell, C. C. M. (1976). Magnetic moments in heusler alloys. *Journal of Magnetism and Magnetic Materials*, *3*(4), 354-360.

Collins, B. A., Chu, Y. S., He, L., Haskel, D. et Tsui, F. (2015). Structural and chemical ordering of Heusler C o x M n y G e z epitaxial films on Ge (111): Quantitative study using traditional and anomalous x-ray diffraction techniques. *Physical Review B*, *92*(22), 224108.

Fariba, N., Mohsen, H., Hossein, M. et Mohsen, K. A. (2015). Study of the structural and magnetic properties and gallium exchange phenomenon in a Mn-Ga alloy doped by Cr during the milling and annealing process. *Journal of Magnetism and Magnetic Materials*, *382*, 271-276.

Felser, C. et Seshadri, R. (2000). Conduction band polarization in some CMR materials: Evolving guidelines for new

systems. *International Journal of Inorganic Materials*, *2*(6), 677-685.

Gani, M., Shah, K. A. et Parah, S. A. (2021). Realization of a Sub 10-nm silicene magnetic tunnel junction and its application for magnetic random access memory and digital logic. *IEEE Transactions on Nanotechnology*, *20*, 466-473.

Graf, T., Felser, C. et Parkin, S. S. P. (2011). Simple rules for the understanding of Heusler compounds. *Progress in solid state chemistry*, *39*(1), 1-50.

Gubin, S. P., Koksharov, Y. A., Khomutov, G. B. et Yurkov, G. Y. (2005). Magnetic nanoparticles: preparation, structure and properties. *Russian Chemical Reviews*, *74*(6), 489.

Holmes, S. N. et Pepper, M. (2002). Magnetic and electrical properties of Co 2 MnGa grown on GaAs (001). *Applied physics letters*, *81*(9), 1651-1653.

Ido, H. (1986). Induced magnetic moment on Co below TC in the ferromagnetic Heusler-type alloys Co2MnX (X= Si, Ge and Sn). *Journal of Magnetism and Magnetic Materials*, *54*, 937-938.

Kämmerer, S., Thomas, A., Hütten, A. et Reiss, G. (2004). Co 2 Mn Si Heusler alloy as magnetic electrodes in magnetic tunnel junctions. *Applied Physics Letters*, *85*(1), 79-81.

Kandpal, H. C., Fecher, G. H. et Felser, C. (2007). Calculated electronic and magnetic properties of the half-metallic, transition metal based Heusler compounds. *Journal of Physics D: Applied Physics*, *40*(6), 1507.

Kim, R. J., Yoo, Y. J., Yu, K. K., Nahm, T., Lee, Y. P., Kudryavtsev, Y. V, Oksenenko, V. A., Rhee, J. Y. et Kim, K. W. (2006). Structural Dependence of the Physical Properties for Co~ 2MnGa Heusler Alloy Films. *JOURNAL-KOREAN PHYSICAL SOCIETY*, *49*(3), 996.

Knowlton, A. A. et Clifford, O. C. (1912). The Heusler alloys. *Transactions of the Faraday Society*, *8*(October), 195-206.

Kobayashi, K., Umetsu, R. Y., Kainuma, R., Ishida, K., Oyamada, T., Fujita, A. et Fukamichi, K. (2004). Phase separation and magnetic properties of half-metal-type Co 2 Cr 1− x Fe x Al alloys. *Applied physics letters*, *85*(20), 4684-4686.

Mahaux, C., Bortignon, P. F., Broglia, R. A. et Dasso, C. H. (1985). Dynamics of the shell model. *Physics Reports*, *120*(1-4), 1-274.

Margulies, D. T., Parker, F. T., Spada, F. E., Goldman, R. S., Li, J., Sinclair, R. et Berkowitz, A. E. (1996). Anomalous moment and anisotropy behavior in Fe 3 O 4 films. *Physical Review B*, *53*(14), 9175.

Miura, Y., Nagao, K. et Shirai, M. (2004). Atomic disorder effects on half-metallicity of the full-Heusler alloys Co 2 (Cr 1− x Fe x) Al: A first-principles study. *Physical Review B*, *69*(14), 144413.

Nazari, F., Hakimi, M., Mokhtari, H., Khajeh Aminian, M. et Esmaeily, A. S. (s. d.). Mn2.

Phong, L. T. H., Manh, D. H., Nam, P. H., Lam, V. D., Khuyen, B. X., Tung, B. S., Bach, T. N., Tung, D. K., Phuc, N. X. et Hung, T. V. (2022). Structural, magnetic and hyperthermia properties and their correlation in cobalt-doped magnetite nanoparticles. *RSC advances*, *12*(2), 698-707.

Raphael, M. P., Ravel, B., Huang, Q., Willard, M. A., Cheng, S. F., Das, B. N., Stroud, R. M., Bussmann, K. M., Claassen, J. H. et Harris, V. G. (2002). Presence of antisite disorder and its characterization in the predicted half-metal Co 2 MnSi. *Physical Review B*, *66*(10), 104429.

Şaşıoğlu, E., Sandratskii, L. M., Bruno, P. et Galanakis, I. (2005). Exchange interactions and temperature dependence of magnetization in half-metallic Heusler alloys. *Physical review B*, *72*(18), 184415.

Varaee, H., Safaeian Hamzehkolaei, N. et Safari, M. (2021). A hybrid generalized reduced gradient-based particle swarm optimizer for constrained engineering optimization problems. *Journal of Soft Computing in Civil Engineering*, *5*(2), 86-119.

Wang, N. (2010). *Fabrication and Integration of permanent magnet materials into MEMS transducers*. University of Florida.

Webster, P. J. et Ziebeck, K. R. A. (s. d.). Alloys and Compounds of d-Elements with Main Group Elements. Part 2 · 1.5.5.4 Dynamics: Datasheet from Landolt-Börnstein - Group III Condensed Matter · Volume 19C: « Alloys and Compounds of d-Elements with Main Group Elements. Part 2 » in SpringerMaterials . Springer-Verlag Berlin Heidelberg. https://doi.org/10.1007/10353201_49

Yin, M., Nash, P. et Chen, S. (2015). Enthalpies of formation of selected Fe2YZ Heusler compounds. *Intermetallics*, *57*, 34-40. https://doi.org/10.1016/J.INTERMET.2014.10.001